

# Solar Spectrum Light-Driven Silicone-Based Fluidic Actuators

Ebrahim Shahabi, Majid Shabani, Fabian Meder,\* and Barbara Mazzolai\*

Soft materials that convert light into mechanical energy can create new untethered strategies for actuating soft robotics. Yet, the available light-driven materials are often incompatible with standard fabrication in soft robotics and restricted to shapes (e.g., sheets) that have limited capability for 3D deformation; often laser or focused light is required for actuation. Here, to address these challenges, a straightforward method for synthesizing sunlight-responsive fluidic actuators from off-the-shelf silicone precursors capable of expanding in 3D is developed. A liquid phase and activated carbon as photothermal elements are constrained in the elastomer. Solar spectral light triggers a liquid–gas phase transition creating sufficient pressure to overcome the internal elastic stress and actuate the material. The fluidic actuation is characterized under varying light conditions reaching expansion cycle times between  $\approx 20$ –500 s, strains of 28%, and actuation stress of  $\approx 1.3$  MPa in different experiments. The materials were then used to exemplarily drive a mechanical switch, a liquid dispensing soft pump, a valve, and a bending actuator. As the described materials are easy to produce in a 5 min synthesis by standard molding techniques, it is believed that they are a promising opportunity for embodied energy converters in environmentally powered soft robots that respond to sunlight.

photosynthesis, phototropisms, and photosymbiosis are examples of well-known mechanisms that respond to or harness sunlight<sup>[7,8]</sup> to achieve growth and biomass, deformations, and other light-controlled reaction cascades in plants and algae.<sup>[9,10]</sup> Realizing light-responsiveness in artificial materials usually requires a combination of mechanisms like light absorption and a subsequent reaction that enables the desired outcome. Light-to-mechanical energy conversion, for example, is especially interesting in achieving autonomous and remotely controlled motion and actuation of robotics and soft robotic systems. Shape changes in soft actuators are typically induced by creating a stress field within the material. By controlling external light irradiation, this stress can become dynamic and change material conditions allowing for reversible actuation. Among the different light-driven actuation mechanisms, photothermal reactions that translate sunlight into heat in the first step are commonly used.


This has several advantages including response to a wide range of wavelengths, high energy conversion efficiency, fast response times, multiple deformation modes, and reversible deformations.<sup>[11]</sup>

The ability of photothermal agents to absorb light and transform it into thermal energy causes local changes in temperature and leads the actuator material to change shape<sup>[12]</sup> by thermal expansion,<sup>[13]</sup> molecular desorption,<sup>[14]</sup> or phase transition.<sup>[15]</sup> A variety of inorganic photothermal agents (such as carbon-based nanomaterials,<sup>[16–19]</sup> plasmonic metallic nanoparticles,<sup>[5,20–24]</sup> semiconductor nanostructures,<sup>[25]</sup> MXenes<sup>[26,27]</sup>) and organic photothermal agents (such as polypyrrole (PPy) organic polymers and polydopamine (PDA)<sup>[28,29]</sup>) have been used in light-driven actuators. The mentioned photothermal agents typically require pairing with thermally responsive matrices to produce light-powered actuators or alternatively photo-isomerization is used.<sup>[30]</sup> These matrices can be soft materials that undergo reversible changes in shape or size in response to temperature changes and include hydrogels,<sup>[23,31,32]</sup> hygroscopic materials,<sup>[24]</sup> shape-memory polymers,<sup>[33,34]</sup> and liquid crystals<sup>[6,35–39]</sup> enabling control over the shape and movement of the actuator material in response to light. Carbon nanomaterials are frequently used as photothermal agents<sup>[40–42]</sup> in light-driven actuation due to their ability to disperse uniformly in the matrix and their strong

## 1. Introduction

Light-responsive materials have a great potential to translate light into mechanical, thermal, electrical, and chemical energy. The photomechanical, thermal, electrical, and chemical conversion can be engineered to operate in the ultraviolet, visible, and near-infrared ranges.<sup>[1–6]</sup> Nature is often inspiration and

E. Shahabi, M. Shabani, F. Meder, B. Mazzolai  
Bioinspired Soft Robotics  
Istituto Italiano di Tecnologia  
Via Morego 30, Genova 16163, Italy  
E-mail: [fabian.meder@iit.it](mailto:fabian.meder@iit.it); [barbara.mazzolai@iit.it](mailto:barbara.mazzolai@iit.it)  
E. Shahabi, M. Shabani  
Biorobotics Institute  
Scuola Superiore Sant'Anna, Pontedera 56025, Italy

 The ORCID identification number(s) for the author(s) of this article can be found under <https://doi.org/10.1002/apxr.202400005>

© 2024 The Authors. Advanced Physics Research published by Wiley-VCH GmbH. This is an open access article under the terms of the [Creative Commons Attribution](#) License, which permits use, distribution and reproduction in any medium, provided the original work is properly cited.

DOI: 10.1002/apxr.202400005

interfacial interaction with the matrix, which can lead to significant improvements in the mechanical properties of the actuator material.<sup>[43]</sup> Yet, a main drawback is that most materials are not commercially available, require complex synthetic procedures, bear toxicity risks, and importantly cannot easily be used in standard fabrication techniques like molding widely used to obtain soft actuators in soft robotics. Indeed, the light-responsive materials often require challenging synthesis and/or result in morphing thin layers that move in a specific direction but do not allow for 3D expansion. In addition, many materials have limited functionality in the spectral range of natural sunlight and respond best with focused, high-intensity UV or IR light sources and lasers.

Here, we are introducing an easy-to-synthesize light-driven soft fluidic actuator. Exposure to light of the natural sunlight spectrum creates internal pressure in the elastic silicone-based matrix capable of 3D expanding the material. The multiphase composite can be fabricated within only 5 min and combines liquid phase-changing materials (here methanol or alternatively ethanol)<sup>[5,44,45]</sup> in an elastomeric matrix (here silicone rubber) together with distributed non-toxic activated carbon particles as photothermal agents. The resulting material can be easily cast and molded like other silicone elastomers into various shapes. Upon light exposure, the photothermal reaction leads to a liquid-gas phase transition creating a pressure in the elastic constraint which expands the soft matrix leading to reversible and multi-cycle actuation. We characterize the thermal kinetics, and the actuation behavior, and present a finite element model that allows to estimate the actuation behavior of different morphologies of the shape-changing materials.<sup>[46]</sup> The ease of synthesis enables rapid prototyping of the actuators with embodied light energy conversion<sup>[47]</sup> as power source. We show this capability by a light-controlled mechanical switching of electrical circuits, autonomous diurnal controlled pumping and dispensing tasks, a valve, and a bending actuator. Such versatile light-driven, moldable soft actuators could especially be interesting for bio- and plant-inspired soft robotics for establishing control mechanisms like circadian rhythms, trigger for example irradiation, and drive structures autonomously by environmental energy without increasing complexity.

## 2. Results and Discussion

### 2.1. Concept and Synthesis of the Light-Responsive Multiphase Composites

One of the main aims of this study was to obtain a light-responsive material that is straightforward to synthesize. Thus, we started creating a multiphase composite from off-the-shelf materials that allow using the sunlight spectrum as a local pressure source leading to material expansion. **Figure 1a** shows the concept: a silicone elastomer hosts distributed inclusions of liquid-to-gas phase transition elements made of methanol and high-surface-area activated carbon particles. Sunlight, especially the near-infrared components, is absorbed by the carbon particles leading to heat generation and photothermal reactions. **Figure S1** (Supporting Information) shows the heating rates of the bare particles as a function of light intensity. The related heat generation is sufficient to evaporate the liquid phase such as methanol (boil-

ing point 64.7 °C) which creates a pressure in the inclusions sufficient to expand the elastomeric matrix. Alternatively, less toxic phase change media could be used as described in the methods section. The process is reversible when not exposed to light due to cooling and condensation as shown later. **Figure 1b** gives an overview of the straight-forward synthetic procedure to obtain the multiphase composite that can be molded into the final actuator shape. The synthesis is completed in typically 5 min followed by  $\approx 10$ -to-15-min curing time, and it enables using standard soft robotic and elastomer molding techniques. **Figure 1c–e** displays the components and the resulting multiphase materials. We used activated charcoal particles with an average size of  $\approx 3.3 \mu\text{m}$  (**Figure 1c**), which can be easily handled in the laboratory (without equipment like glove boxes, etc., recommended for the use of carbon nanopowders), and distributed them in different densities in the silicone elastomer by varying their concentration during step 3 of the synthesis.

**Figure 1d** shows resulting actuators with different particle concentrations, here molded in cylindrical shapes. One of the best actuation behaviors, as detailed later, has been achieved by  $\approx 1$  wt.% of activated charcoal particles and **Figure 1e** shows a digital microscopy of this composite in which the distribution of the darker carbon particles in the elastic matrix can be observed (the zoomed-in inset shows an inclusion of the liquid methanol phase).

### 2.2. Embodied Light-to-Heat Energy Conversion

**Figure 2** summarizes the light-to-heat and heat-to-pressure energy conversion capability of multiphase materials. **Figure 2a** shows the reversible heating and cooling kinetics during on–off switching of the lamp that excites the sample with the standard solar spectrum AM1.5G. When the sample (1 wt.% carbon particles) is exposed to light, it rapidly heats up, initially with a linear slope of 0.34 °C per second then slowing down and reaching a maximum overall temperature of  $\approx 53$  °C. After switching the light source off, the composite rapidly cools down with initially a linear behavior and a cooling rate of 0.27 °C per second until  $\approx 30$  °C followed by a non-linear slower cooling phase. For actuation capability, the corresponding vapor pressure of the methanol is important and **Figure 2a** plots the variation in the vapor pressure in mbar showing that the particle-light interaction and corresponding heating and cooling phases can lead to a pressure change of  $>400$  mbar. **Figure 2b** indicates that the heating rate is expectedly dependent on the amount of carbon particles in the final multiphase system and particle concentrations below 1 wt.% led to slower heating and reduced maximum temperatures. Above a concentration of 1 wt.%, no significant further enhancement has been observed, so 1 wt.% was chosen for further experiments. Videos **S1** and **S2** (Supporting Information) show the dynamic temperature variation under exposure to 155 mW cm<sup>-2</sup> light irradiation and the vertical deformation of the soft multiphase materials in a cylindrical rigid constrain as a function of particle concentration, respectively visualizing the effect of particle content on heating and actuation. The results given in **Figure 2c** confirm instead that the light intensity expectedly has an influence on the temperature variation and the highest heating rate was found at 0.4 °C s<sup>-1</sup> at the highest

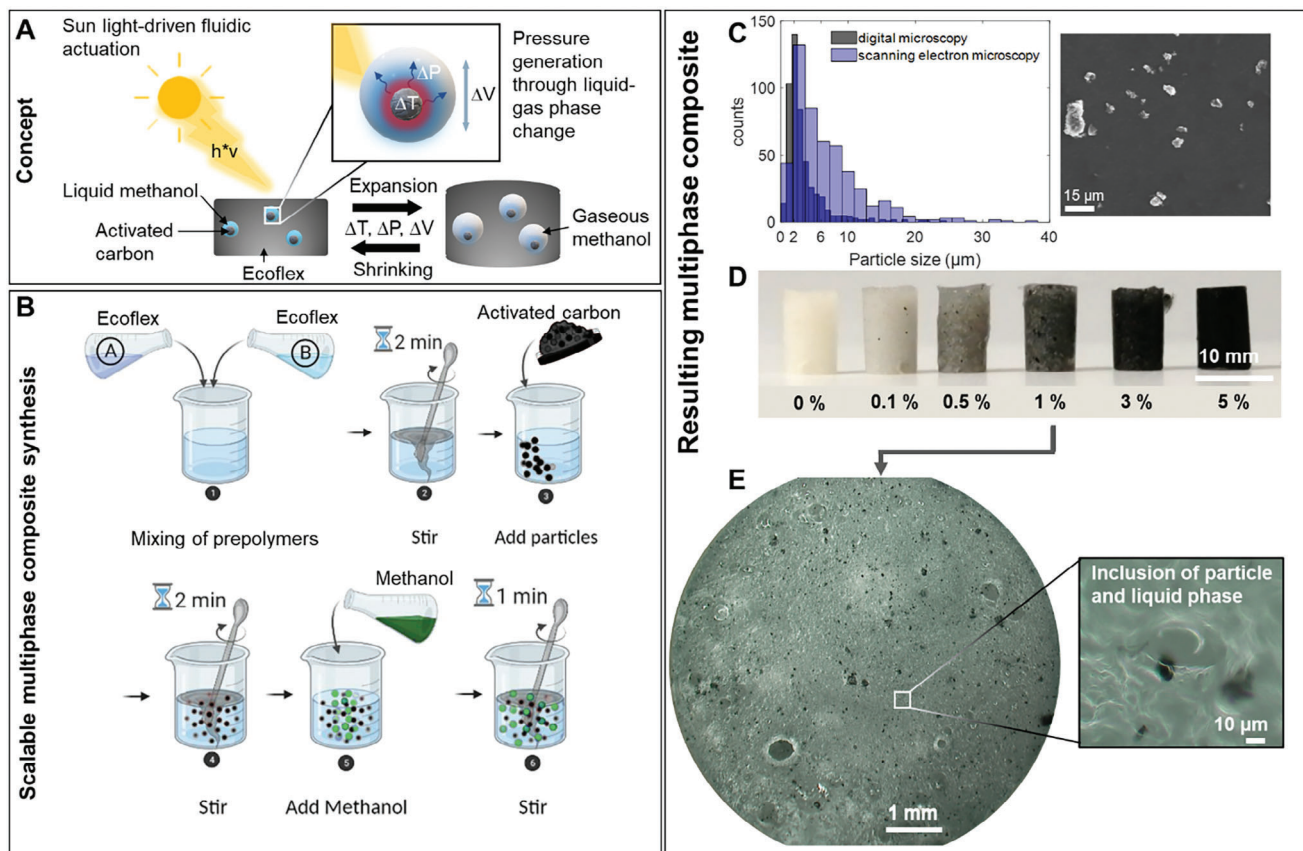


**Figure 1.** Concept, synthesis, and resulting multiphase materials for enabling solar spectrum light-driven fluidic actuation. A) Schematic of the light-to-mechanical energy conversion based on the reversible liquid-to-gas phase change driven by photothermal reaction of distributed activated carbon particles and liquid methanol inclusions. B) Straightforward 5-minute synthetic procedure using off-the-shelf materials methanol, activated carbon (powdered Norit RB3), and Ecoflex 00–35 fast curing silicone elastomer. C) Scanning electron microscopy (SEM) image and particle distributions (SEM and digital microscopy, see Figure S2, Supporting Information) of the photothermal carbon particles with an average diameter of  $\approx 3 \mu\text{m}$ . D) Resulting, soft multiphase actuators molded in a cylindrical shape with varying particle concentration in wt.%; other shapes can easily be obtained using other molds. E) Zoom-in on the top-view of the cylindrical actuator with 1 wt.% carbon particles showing inclusions of carbon particles and liquid phase (inset).

intensity. Outdoor sun radiation on a sunny day in June at noon at our headquarters ( $44^\circ 28' 30,07'' \text{ N}$ ,  $8^\circ 54' 22,65'' \text{ E}$ ) was  $103 \text{ mW cm}^{-2}$  and Video S3 (Supporting Information) shows the deformation of a randomly shaped soft multiphase material with 1 wt.% carbon particles under natural sunlight radiation. Further characteristics of the solar simulator and its tunability are given in Figure S3 (Supporting Information). The characterization indicates that the light-to-heat conversion by the carbon particles leads to a significant variation in temperature and the liquid phase's vapor pressure in typically  $< 60 \text{ s}$ . As the measurements by thermal imaging give information on the overall temperatures of the multiphase materials, the local temperatures in proximity to the carbon particles might be significantly larger. In addition, the silicone elastomer and methanol phase (and the phase change) will influence the overall temperature distribution, and tuning liquid phase and heat exchange with the matrix and the environment could be tools to further tune the behavior such as locally increasing heat transfer.<sup>[48]</sup>

As function of temperature and boiling point of the solvent, the vapor pressure varies as described by Antoine's equation and in case methanol should be replaced with a less toxic solvent

like ethanol (see Experimental Section), a variation in the pressure generation can be accordingly estimated. The vapor pressure curves for ethanol at temperatures generated by the carbon particles under light excitation are given in Figure S4 (Supporting Information) and compared with methanol. Moreover, the actual pressure changes that the actuator can exert through its volume expansion is a different parameter that is interesting for example for applications like pumps and valves. Thus, we measured the pressure change, the actuator can exert in a closed environment during light excitation and actuation  $\Delta P_{\text{act}}$  in Figure 2d. To do so, a piece of the multiphase material with a volume of  $1070 \text{ mm}^3$  was placed in a rigid chamber (volume  $1340 \text{ mm}^3$ ) equipped with a pressure sensor to directly measure pressure variation due to actuation of the material under light on-off cycles. The measured pressure changes are a result of the collective phase transitions of the multiple methanol-filled cavities distributed in the elastic matrix, the deformation of the elastic matrix, and the compression of the remaining external gas phase in the measurement chamber. Thus, the pressure variation depends on parameters like the chamber dimensions and multiphase material composition. The mean pressure variation rate during light-on cycles using

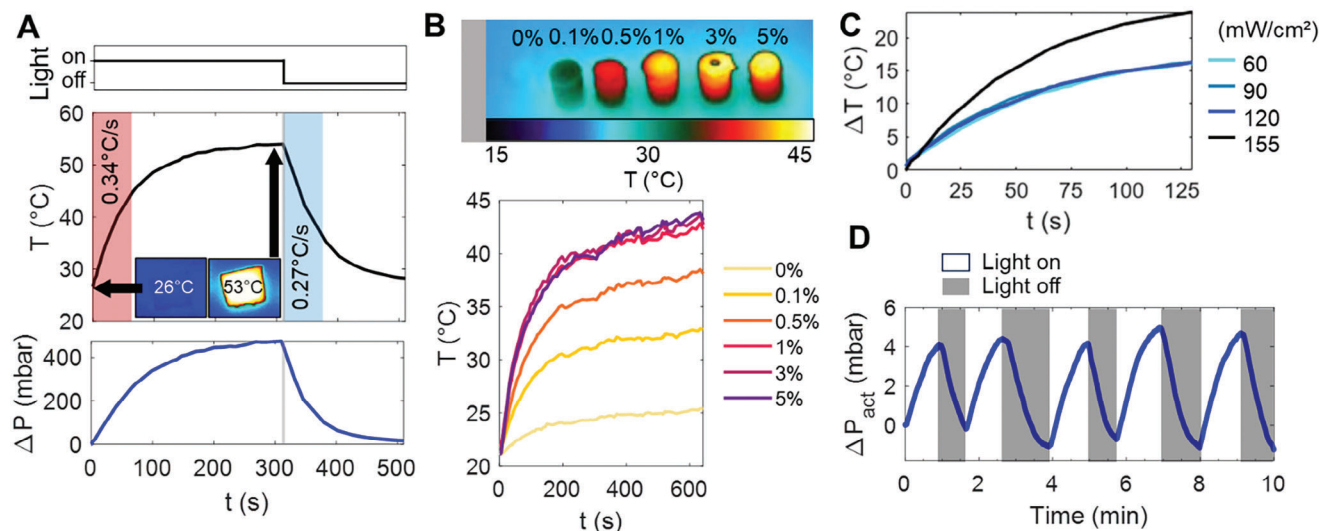


**Figure 2.** Light-to-heat energy conversion properties of the multiphase materials. A) Reversible heating and cooling kinetics of a composite with 1 wt.% carbon particles under simulated sunlight ( $1.55 \text{ mW cm}^{-2}$ , AM1.5G spectrum) recorded by thermography. The red and blue bars show the ranges of linear progression with indicated heating and cooling rates of  $0.34$  and  $0.27 \text{ °C s}^{-1}$ , respectively. The insets show the thermal images of a rectangular sample after the indicated exposure times. The lower panel shows the predicted pressure variation as a function of temperature change due to evaporation of methanol calculated by Antoine's equation (Figure S4, Supporting Information). B) Light-to-heat conversion kinetics as a function of carbon particle concentration in wt.% in the multiphase materials (maintaining a constant silicone and methanol content). The top thermography image shows the heat distribution as a function of carbon particle concentration at  $t = 600 \text{ s}$ . C) Variation of the temperature  $\Delta T$  of the multiphase materials as a function of exposed light power, AM1.5G spectrum. D) Pressure variation of the actuator  $\Delta P_{\text{act}}$  measured during expansion and shrinkage of the multiphase material (volume  $1070 \text{ mm}^3$ ) during light on-off cycles in a closed rigid chamber (volume  $1340 \text{ mm}^3$ ). All experiments have been performed in environments with temperatures between  $22\text{--}26 \text{ °C}$ .

multiphase material with 1 wt.% carbon particles were  $1.24 \pm 0.14$  and  $1.58 \pm 0.19 \text{ mbar min}^{-1}$  during light-off cycles, respectively. A mean maximal pressure variation of  $\approx 4 \text{ mbar}$  per cycle was achieved corresponding to an actuation stress of  $1.34 \text{ MPa}$  exerted on the membrane of the pressure sensor (area  $\approx 3 \text{ mm}^2$ ) during light-on cycles. Figure S5 (Supporting Information) compares the performance of our actuators with other light-driven actuators revealing an outstanding stress and strain performance.

### 2.3. Light-Driven Actuation of the Multiphase Materials

Figure 3 displays the actuation behavior and the expansion of the elastic matrix of the multiphase composites due to the heat-induced liquid-to-gas phase transition. The actuation depends on the shape of the final material which can be easily varied, by standard molding techniques or cutting casted material into the desired shape. Figure 3a shows exemplarily the expansion of the central point of an actuator with the shape of a spherical cap obtained by curing a drop of the multiphase material with a volume of  $1.25 \text{ mL}$  on a rigid surface. Actuation is initiated by exposure to the  $155 \text{ mW cm}^{-2}$  ( $\approx 1.5 \text{ sun}$ ) followed by subsequent exposure to dark conditions as indicated. The actuator deforms in three dimensions but is constrained at its bottom due to the rigid support. We track the vertical deformation of the actuator as explained in the figure and it rapidly increases (correlating with the temperature profiles), then slows down and reaches a maximum at  $\approx 128\%$  deformation, ( $28\%$  strain). Subsequently, when the light source is turned off, the initial configuration is reestablished during cooling and heat dissipation into the environment

(room temperature  $25 \text{ °C}$ ). It reaches rapidly (within  $\approx 150 \text{ s}$ ) almost its original state ( $103\%$  vertical deformation) while the full recovery of the initial shape takes  $\approx 370 \text{ s}$ , the whole cycle is shown in Video S4, Supporting Information). Figure 3b plots the vertical deformation as a function of temperature showing that the curves for the heating and cooling cycles almost overlap. This confirms cycle reversibility, and that the light-induced temperature variation (and the resulting material-internal evaporation and condensation reactions) is as expected the driving force for the material actuation.

Moreover, we implemented a finite-element model of the light-induced actuation behavior to estimate the expansion behavior as a function of the shapes of the multiphase materials. Figure 3 shows examples of the simulated shapes predicted to produce standard deformation typically shown with light-driven actuators like grasping or bending actuation even if those are not specifically main application target of our actuators. Other applications as described later are more interesting. A stomata-like valving behavior for example can be obtained by combining two spherical caps and this could be interesting to control water flow depending on sunlight exposure. Detailed information on the model is given in Figures S6–S10 and Video S5 (Supporting Information) shows an overview of the simulated dynamic motion. Instead, Videos S6 and S7 (Supporting Information) show the experimental implementation of a bending actuation and a valve operating in a similar manner as projected by the model. Yet, the model was not used and intended to fully predict and describe the actuators' behavior but to take design decisions for the structural components useful to create certain motion patterns. It helps to estimate how introducing gradients or stiffness variations could

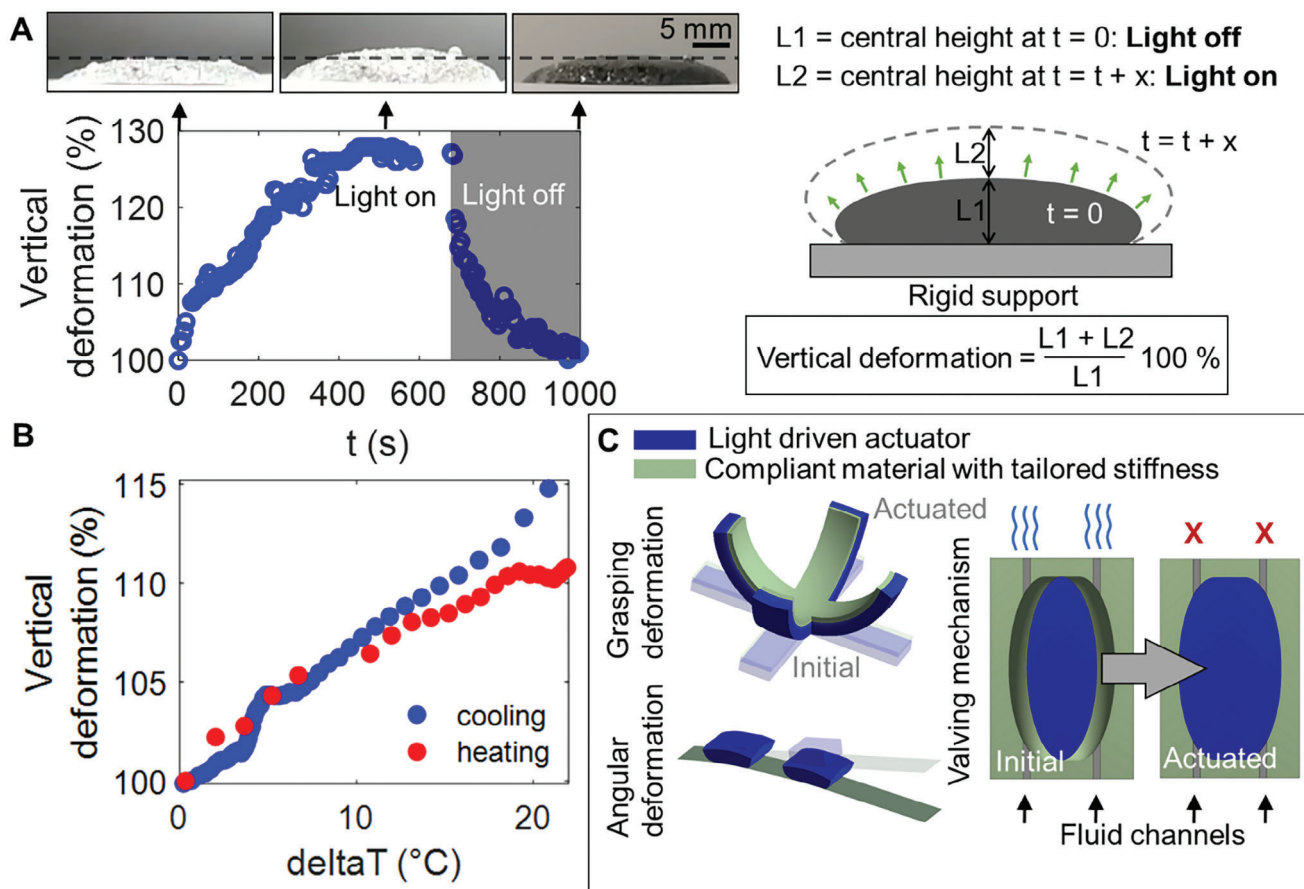


**Figure 3.** Light-driven actuation by conversion of light into elastic expansion. A) Time-resolved light-driven vertical deformation of a spherical cap of the multiphase materials during light on-off phases ( $155 \text{ mW cm}^{-2}$ , 1.5 sun, AM1.5G spectrum). To demonstrate the 3D deformation, the vertical deformation (in z-direction) was video-tracked and calculated as indicated in the schematic and formula on the right (images show video frames at time points indicated by the arrows). B) Vertical deformation as a function of temperature variation  $\Delta T$  during heating (red) and cooling (blue) cycles. C) Simulation of the dynamic deformation allows to predict and project more complex motion trajectories; here a typical grasper, an angular bending deformation through two actuators, and a stomata-inspired fluid channel valving mechanism by combining actuator materials (blue) with materials of tailored stiffness (details in Supporting Figures S6–S10 and Video S5, Supporting Information).

lead to more complex behaviors that are shapeable to the desired application before performing the experimental implementation.

A benefit of our material system is the opportunity to mold different 3D shapes, and typical constraints of light-driven actuators such as limitation to sheet-like bending deformation, complex fabrication, or limited quantity of the final materials, which are no constraints for our system. Fluidic actuation by pressurized elastomers is a versatile actuation mechanism in soft robotics with multiple advantages like lightweight structures, no rigid parts required, higher degree of freedom, etc. that in our case can also be driven in an untethered manner by solar spectrum light.

#### 2.4. Demonstration of Light-Driven Pumping and Switching Systems

Here, we demonstrate the actuation capability with two further examples in more detail, a light-driven mechanical switch that is used to control an electric circuit in response to light (Figure 4a)

and a soft, light-driven pump that enables to autonomously dispense liquids from a reservoir driven by light in the solar spectrum (Figure 4b–d). Figure 4a shows the circuit that is controlled by two metallic contacts which are kept separated by the expansion of the actuated multiphase material in light. The switch closes the circuit in darkness and controls a light-emitting diode (LED). The reversible multicycle switching is shown in Figure 4a, and it can be observed that rapidly after the light source driving the actuator is turned off, the green LED switches on (with a mean switching rate of  $20 \pm 4$  s). The process is reversible when the light exciting the actuator is turned on showing the repeatability of the process and LED switches off with a mean switching rate of  $93 \pm 31$  s. Video S8 (Supporting Information) shows the behavior. The switching rates are thereby obviously faster than the circadian rhythm which could be envisioned as autonomous control of the actuator as discussed further later (for 12 h light periods, 43 200 s, LED-off switching is  $\approx 460$  times faster, LED-on switching 2160 times faster).

Nevertheless, the fluidic actuation mechanism allows also for more complex tasks such as autonomous pumping in a

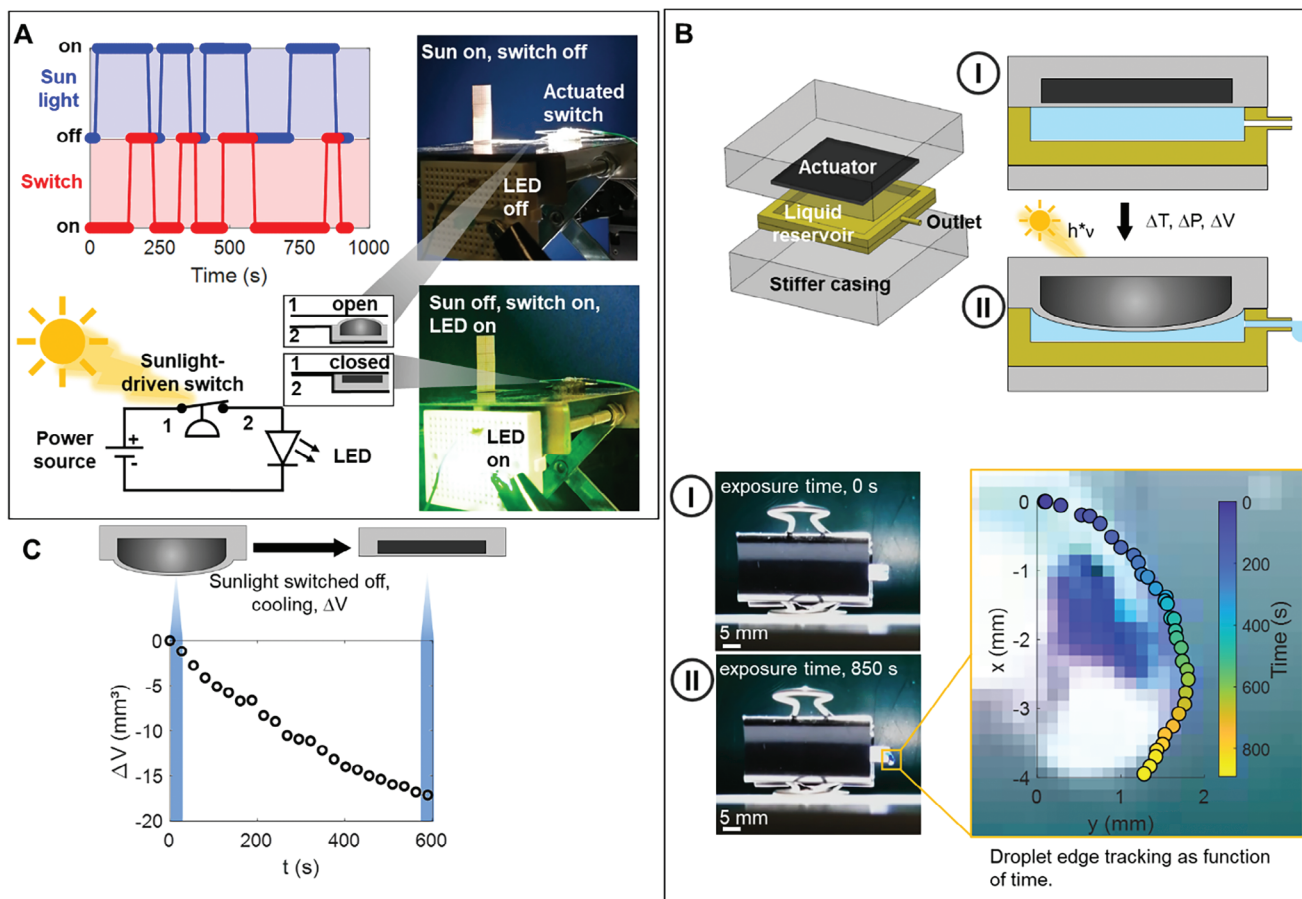


**Figure 4.** Demonstration of a solar spectrum light-driven mechanical switch and autonomous pumping structure. A) Multicycle on-off alternation of a light-driven analog switch controlling an LED light using the circuit indicated in the figure. The multiphase material controls the contact between two conductors keeping the switch open during light exposure whereas it quickly closes in darkness switching the green LED on (Video S7, Supporting Information shows the multicycle operation of the light-controlled circuit). B) Design, components, and actuation mechanism of an autonomous light-driven water dispensing system. Expansion of the multiphase material during light exposure increases the pressure in the liquid reservoir driving it to the outlet. (Video S8, Supporting Information shows the light-driven water dispensing). The lower images are side-view images of the pumping system and time-resolved tracking of the dispensing droplet edge during light exposure. C) Time-resolved negative volume change ( $\Delta V$ ) during the cooling phase (in darkness) after previous expansion in light representing the suction force during the cooling phase, generating a flow rate of  $2.25 \mu\text{L min}^{-1}$ . Light power was set to  $155 \text{ mW cm}^{-2}$  (AM1.5G spectrum) in both cases.

straightforward configuration. The assembly of the pumping system using the same multiphase material is displayed in Figure 4b. The device consists of a  $10 \times 10 \times 2.5 \text{ mm}$  casted multiphase actuator (depicted in black) which is inserted in a liquid chamber (light blue) containing the reservoir of the liquid to be dispensed and a stiffer, non-elastic glass case (grey). Exposure to light heats the multiphase material through the glass case leading to expansion within the liquid reservoir. This dispenses the liquid (here dyed water) through the outlet Figure 4b also shows the side view of the dispensing system and the tracking of the droplet edge as a function of light-exposure time at  $155 \text{ mW cm}^{-2}$  (Video S9, Supporting Information shows the autonomous pumping). Figure 4d instead plots the negative volume change ( $\Delta V$ ) during the cooling phase when the sunlight simulator is turned off and the expanded multiphase material ( $t = 0$ ) cools down reaching  $\approx 18 \text{ mm}^3$  (corresponding to 7.2% of the initial volume of the actuator) generating a flowrate of  $2.25 \mu\text{L min}^{-1}$ .

This shows that not only pumping could be realized but the negative pressure occurring during the cooling phase may be used as suction force in a more complex configuration in which valves (that may also be light-driven<sup>51</sup>) could act as control units for precise microvolume dispensing and suction.

The experiments clearly show the potential of the light-responsive, silicone-based composites to realize actuators that can be autonomously controlled by the diurnal rhythm (simulated here by on-off switching of the light source). In a practical scenario, this means one on-off cycle per day and applications like switching lighting or irrigation of plants by pumps and partially anticipated by the demonstrators in this study could benefit from the actuation systems. More complex control including the activation of reflective surfaces or shading elements when certain expansion is reached could be a tool to achieve multiple cycles during a day in future. Detailed outdoor tests that consider variable weather conditions, cooling by wind, and sunlight

intensity changes need to be conducted to further design the materials in specific application scenarios. Those investigations should better assess the long-term operability and reversibility, for example, evaluating a potential need to reconstitute the liquid phase after certain operation periods. Further improvements in the materials and the functionality may be achieved by exploring different liquid phases (with different boiling points and liquid-matrix interactions), by tailored shapes and stiffness gradients, and by tailoring heat exchange between the environment and elastic matrix.

### 3. Conclusion

Here we present an easy-to-synthesize light-driven fluidic actuator operating in the solar spectrum for soft robotic applications. The actuators can be obtained by combining off-the-shelf materials into a multiphase material in a 5-minute synthesis and cast and molded like other silicone elastomers which gives the opportunity to easily obtain various shapes. The actuating multiphase material allows for autonomous diurnal switching due to an internal liquid-gas phase transition but is significantly faster than the diurnal rhythm reaching the regime of maximum expansion in a typical 20–500 s depending on configuration and application. We believe that the easy synthesis and flexibility of the manufacturing process allow to exploit this material in multiple applications, especially in environmentally driven soft and bioinspired robotics.

### 4. Experimental Section

**Materials:** Steam-activated charcoal pellets Norit RB3, and methanol, purity of 99.8% were purchased from Sigma-Aldrich, Italy, and used as received. The activated carbon particles were manually ground with a pestle in a mortar for a period of 5 min to reduce the particle size to  $\approx 1$  and  $50 \mu\text{m}$  and an average of  $3.3 \mu\text{m}$ . The silicone elastomer, Ecoflex 00–35 fast (pot life 2.5 min, curing time is 5 min) was purchased from Smooth-On (USA) and used as received.

**Synthesis of Light-Responsive Multiphase Composites:** The entire synthetic process took 5 min. First, equal amounts of the parts A and B of the Ecoflex 00–35 fast prepolymer (typically 5 g + 5 g) were mixed and stirred with a rod for one minute. After that, a suspension of carbon particles (in the desired wt.% relative to the total weight of the elastomer) mixed in 2 mL methanol was immediately added to elastomer precursors, and the mixture was manually stirred with a rod for 30 s. Then, 1 mL of pure methanol was added and mixed for another minute. The methanol slightly increases the pot life, but it was important to maintain short mixing times to avoid a too-quick polymerization of the elastomer. The mixture was poured into a mold or cast into a film and left at room temperature for typically 20 min before usage. The schematic process of manufacturing is shown in Figure 1B. Whereas the activated carbon particles and Ecoflex 00–35 were not classified as hazardous or toxic substances (the readers are referred to the materials safety data sheets, MSDS), it is advisable to avoid exposure to particle dust and its inhalation during the synthesis, for example by respiration protection or fume hood. Instead, methanol is a hazardous substance that is toxic by ingestion, skin penetration, and inhalation, and it must be handled carefully as reported in the MSDS using the suggested safety and protection measures. Higher quantities (a few mL) were used only during the actuator preparation phase but also in the final actuators, methanol is encapsulated in the silicone matrix even if in small volumes. Thus, users should be aware that it might permeate through the silicone matrix and cause a possible exposure originating from the final actuators. It is suggested to readers that aim to replicate the actu-

ators and cannot work under the safety standards necessary for handling methanol as reported in the MSDS, to replace methanol with less critical alcohols like ethanol (slightly higher boiling point and slightly lower vapor pressure, see Figure S4, Supporting Information but less toxic)<sup>[49]</sup> or other low toxicity low boiling point liquids.

**Instrumentation and Characterization:** An AAA class SciSun 300 Solar Simulator (Sciencetech Inc., Canada) was used to replicate the AM1.5G standard spectrum in the UV–VIS–IR spectral range with class AAA specification (according to ASTM E927-19 and IEC-60904-9) with the option to vary the power and control intensity between 0 up to  $155 \text{ mW cm}^{-2}$  and an exposure area of  $5 \text{ cm}^2$ . An IR thermal camera (A700, FLIR Systems, USA) was used to record the temperature profiles and heating–cooling rates of the light-exposed–unexposed composite materials. The recorded data were analyzed using the software package ResearchIR (Version 4.40.12.38, FLIR Systems, USA). Power densities of the simulated sunlight were measured using an RS PRO IM 750 Solar Power Meter (RS, UK). A KH-8700 digital microscope (Hirox, Japan) was used to measure particle sizes and image the multiphase composites. Scanning Electron Microscopy (SEM) images were taken using an EVO MA10 (Zeiss, Germany). The pressure changes that the multiphase material can exert through expansion was measured in a self-made rigid and fully sealed measurement chamber equipped with a borosilicate glass window for sample excitation and a differential analog pressure sensor (010MDAA5, TruStability, Honeywell, USA) read-out using a NI USB-6009 (National Instruments, USA). The data were analyzed in MATLAB (Version 2022b).

**Fabrication of the Light-Controlled Analog Switch and Liquid Dispensing/Pumping System:** Two applications are shown in detail using the light-driven actuator. The electrical circuit was made of standard components, a green LED, and a 3 V power supply. The sphere cap-shaped actuator with a diameter of 15 mm was mounted between two metal electrodes in a manner that the electrodes made contact when the actuator was in its intrinsic state and the electrodes separated when it was expanded during light exposure, closing the circuit only when the actuator was not expanded. The pumping device consists of four parts: the top, bottom, liquid reserve, and actuator  $10 \times 10 \times 2.5 \text{ mm}$  cast multiphase actuator. The top and bottom closures ( $50 \times 50 \text{ mm}$ ) were laser-cut from a 5 mm thick acrylic sheet using a VersaLaser VLS3.60 (Universal Laser Systems Inc., USA). The liquid reservoir was laser cut from a 1.5 mm thick silicone rubber sheet as a base plate and a frame to which a silicone tubing was glued with Sil-Poxy adhesive (Smooth-On, USA) as an outlet. The actuator was put in the frame of the central part sitting on the bottom part and the liquid (blue-stained water) was filled in the remaining space. Then the top closure was added and fixed with mechanical clamps keeping the different layers firmly sealed.

**Simulation of the Material Behavior:** To analyze and predict the behavior of the developed sunlight-driven material, finite element method (FEM) simulations using ANSYS Workbench 19.2 were employed, simulating the photothermal reaction and expansion of the actuator by introducing a temperature increment in an elastically deforming specimen. Further details can be found in Figures S5–S9 of the Supporting Information.<sup>[50–53]</sup>

### Supporting Information

Supporting Information is available from the Wiley Online Library or from the author.

### Acknowledgements

E.S., M.S., and F.M. contributed equally to this work. The authors thank Serena Armiento for taking SEM images of the activated charcoal particles. This work was carried out within the framework of the project “RAISE-Robotics and AI for Socioeconomic Empowerment” and has been supported by European Union- Next Generation EU.

### Conflict of Interest

The authors declare no conflict of interest.

## Data Availability Statement

The data that support the findings of this study are available from the corresponding author upon reasonable request.

## Keywords

autonomous soft robotics, bioinspired robotics, embodied energy, multi-phase composites, phase transitions, photoresponsive materials, soft actuation, sunlight-driven actuation

Received: March 12, 2024

Revised: April 8, 2024

Published online: June 11, 2024

- [1] T. Sasaki, J. M. Tour, *Org. Lett.* **2008**, *10*, 897.
- [2] B. Han, Y. L. Zhang, Q. D. Chen, H. B. Sun, *Adv. Funct. Mater.* **2018**, *28*, 1802235.
- [3] S. V. Ahir, E. M. Terentjev, *Nat. Mater.* **2005**, *4*, 491.
- [4] T. Zhang, H. Chang, Y. Wu, P. Xiao, N. Yi, Y. Lu, Y. Ma, Y. Huang, K. Zhao, X. Q. Yan, Z. B. Liu, J. G. Tian, Y. Chen, *Nat. Photonics* **2015**, *9*, 471.
- [5] F. Meder, G. A. Naselli, A. Sadeghi, B. Mazzolai, *Adv. Mater.* **2019**, *31*, 1905671.
- [6] S. Li, M. M. Lerch, J. T. Waters, B. Deng, R. S. Martens, Y. Yao, D. Y. Kim, K. Bertoldi, A. Grinthal, A. C. Balazs, J. Aizenberg, *Nature* **2022**, *605*, 76.
- [7] A. Stirbet, D. Lazár, Y. Guo, G. Govindjee, *Ann. Bot.* **2020**, *126*, 511.
- [8] G. D. Stanley, *Science* **2006**, *312*, 857.
- [9] J. P. Vandenbrink, E. A. Brown, S. L. Harmer, B. K. Blackman, *Plant Sci* **2014**, *224*, 20.
- [10] M. J. Correll, J. Z. Kiss, *J. Plant Growth Regul.* **2002**, *21*, 89.
- [11] M. Yang, Z. Yuan, J. Liu, Z. Fang, L. Fang, D. Yu, Q. Li, *Adv. Opt. Mater.* **2019**, *7*, 1900069.
- [12] Y. Chen, J. Yang, X. Zhang, Y. Feng, H. Zeng, L. Wang, W. Feng, *Mater. Horiz.* **2021**, *8*, 728.
- [13] Z. Tang, Z. Gao, S. Jia, F. Wang, Y. Wang, *Adv. Sci.* **2017**, *4*, 1600437.
- [14] M. Ji, N. Jiang, J. Chang, J. Sun, *Adv. Funct. Mater.* **2014**, *24*, 5412.
- [15] H. Ma, X. Xiao, X. Zhang, K. Liu, *J. Appl. Phys.* **2020**, *128*, 101101.
- [16] I. Vassalini, I. Alessandri, *Nanoscale* **2017**, *9*, 11446.
- [17] C. Lin, Y. Zhu, *Appl. Opt.* **2016**, *55*, 2324.
- [18] Y. Yu, L. Li, E. Liu, X. Han, J. Wang, Y. X. Xie, C. Lu, *Carbon* **2022**, *187*, 97.
- [19] L. Chang, D. Wang, Z. Huang, C. Wang, J. Torop, B. Li, Y. Wang, Y. Hu, A. Aabloo, *Adv. Funct. Mater.* **2023**, *33*, 2212341.
- [20] C. Zheng, F. Jin, Y. Zhao, M. Zheng, J. Liu, X. Dong, Z. Xiong, Y. Xia, X. Duan, *Sens. Actuators, B* **2020**, *304*, 127345.
- [21] E. Lee, D. Kim, H. Kim, J. Yoon, *Sci. Rep.* **2015**, *5*, 15124.
- [22] A. Nishiguchi, H. Zhang, S. Schweizerhof, M. F. Schulte, A. Mourran, M. Möller, *ACS Appl. Mater. Interfaces* **2020**, *12*, 12176.
- [23] H. Zhang, H. Zeng, A. Eklund, H. Guo, A. Priimagi, O. Ikkala, *Nat. Nanotechnol.* **2022**, *17*, 1303.
- [24] S. Mariani, L. Cecchini, A. Mondini, E. Del Dottore, M. Ronzan, C. Filippeschi, N. M. Pugno, E. Sinibaldi, B. Mazzolai, *Adv. Mater. Technol.* **2023**, *n/a*, 2202166.
- [25] Y. Song, B. Cretin, D. M. Todorovic, P. Vairac, *J. Phys. Appl. Phys.* **2008**, *41*, 155106.
- [26] L. Xu, F. Xue, H. Zheng, Q. Ji, C. Qiu, Z. Chen, X. Zhao, P. Li, Y. Hu, Q. Peng, X. He, *Nano Energy* **2022**, *103*, 107848.
- [27] J. Liu, L. Xu, Q. Ji, L. Chang, Y. Hu, Q. Peng, X. He, *Adv. Funct. Mater.* **2024**, *34*, 2310955.
- [28] T. Wang, M. Li, H. Zhang, Y. Sun, B. Dong, *J. Mater. Chem. C* **2018**, *6*, 6416.
- [29] C. Lee, J. H. Park, M. Kim, J. S. Kim, T. S. Shim, *Soft Matter* **2022**, *18*, 4604.
- [30] M. R. A. Bhatti, A. Kernin, M. Tausif, H. Zhang, D. Papageorgiou, E. Bilotti, T. Peijs, C. W. M. Bastiaansen, *Adv. Opt. Mater.* **2022**, *10*, 2102186.
- [31] Y. Cao, W. Li, F. Quan, Y. Xia, Z. Xiong, *Front. Mater.* **2022**, *9*, 827608.
- [32] L. Yang, T. Zhang, W. Sun, *J. Appl. Polym. Sci.* **2020**, *137*, 49375.
- [33] S. Li, X. Jin, Y. Shao, X. Qi, J. Yang, Y. Wang, *Eur. Polym. J.* **2019**, *116*, 302.
- [34] Y. Xia, Y. He, F. Zhang, Y. Liu, J. Leng, *Adv. Mater.* **2021**, *33*, 2000713.
- [35] P. Rastogi, J. Njuguna, B. Kandasubramanian, *Eur. Polym. J.* **2019**, *121*, 109287.
- [36] T. J. White, D. J. Broer, *Nat. Mater.* **2015**, *14*, 1087.
- [37] M. Pilz da Cunha, M. G. Debije, A. P. H. J. Schenning, *Chem. Soc. Rev.* **2020**, *49*, 6568.
- [38] H. Zeng, P. Wasylczyk, D. S. Wiersma, A. Priimagi, *Adv. Mater.* **2018**, *30*, 1703554.
- [39] H. Zeng, O. M. Wani, P. Wasylczyk, R. Kaczmarek, A. Priimagi, *Adv. Mater.* **2017**, *29*, 1701814.
- [40] X. Wang, N. Jiao, S. Tung, L. Liu, *ACS Appl. Mater. Interfaces* **2019**, *11*, 30290.
- [41] W. Jiang, D. Niu, H. Liu, C. Wang, T. Zhao, L. Yin, Y. Shi, B. Chen, Y. Ding, B. Lu, *Adv. Funct. Mater.* **2014**, *24*, 7598.
- [42] Y. Hu, J. Liu, L. Chang, L. Yang, A. Xu, K. Qi, P. Lu, G. Wu, W. Chen, Y. Wu, *Adv. Funct. Mater.* **2017**, *27*, 1704388.
- [43] Y. Huang, Q. Yu, C. Su, J. Jiang, N. Chen, H. Shao, *Actuators* **2021**, *10*, 298.
- [44] X. Li, H. Duan, P. Lv, X. Yi, *Soft Robot* **2020**, *8*, 251.
- [45] A. Miriyev, K. Stack, H. Lipson, *Nat. Commun.* **2017**, *8*, 596.
- [46] L. Marechal, P. Balland, L. Lindenroth, F. Petrou, C. Kontovounisios, F. Bello, *Soft Robot.* **2020**, *8*, 3.
- [47] C. A. Aubin, B. Gorissen, E. Milana, P. R. Buskohl, N. Lazarus, G. A. Slipher, C. Keplinger, J. Bongard, F. Iida, J. A. Lewis, R. F. Shepherd, *Nature* **2022**, *602*, 393.
- [48] M. D. Bartlett, N. Kazem, M. J. Powell-Palm, X. Huang, W. Sun, J. A. Malen, C. Majidi, *Proc. Natl. Acad. Sci* **2017**, *114*, 2143.
- [49] Dortmund Data Bank, <https://www.ddbst.com> (accessed: December 2023).
- [50] Y. Elsayed, A. Vincensi, C. Lekakou, T. Geng, C. M. Saaj, T. Ranzani, M. Cianchetti, A. Menciassi, *Soft Robot* **2014**, *1*, 255.
- [51] F. Connolly, P. Polygerinos, C. J. Walsh, K. Bertoldi, *Soft Robot* **2015**, *2*, 26.
- [52] P. Bing, X. Hui-min, H. Tao, A. Asundi, *Polym. Test.* **2009**, *28*, 75.
- [53] T. I. Lee, M. S. Kim, T. S. Kim, *Polym. Test.* **2016**, *51*, 181.